A Model for Time Dependent Strain Accumulation and Damage at Low Temperatures in Ti-6Al-4V

W. J. Harrison, M. T. Whittaker and R. Lancaster
Swansea University, Singleton Park, Swansea, SA2 8PP

Abstract
Dwell fatigue effects at low temperatures in a range of titanium alloys have been well documented since the 1970s. However, attempts to model dwell fatigue phenomena are limited. The time dependent effects have been shown to be due to the inherent strain accumulation behaviour at ambient or low temperatures, loosely termed 'cold creep' in alloys such as Ti-6Al-4V. Periods of dwell in a fatigue cycle or the application of a high mean stress not only cause stress relaxation, but can lead to premature failures characterised by quasi-cleavage facets under certain conditions. The conditions under which these facets form are not fully understood.
This paper introduces a method for predicting cold creep in Ti-6Al-4V by attempting to quantify time dependent deformation and rupture caused by the formation of quasi-cleavage facets observed in this titanium alloy. A logarithmic creep method has been used to describe low temperature creep curves. However this method fails to predict the curve shape at higher stresses. An additional term is used to quantify creep rates at all conditions. A finite element model has been developed, based on this method, which accurately predicts stress relaxation at ambient temperature and quantifies time dependent failure in a notched specimen under cyclic loading.

1. Introduction

Two phase α+β titanium alloys are widely used in gas turbine aero engines due to a combination of their high strength to weight ratio, good fatigue properties at low to medium temperatures and good fracture toughness. Their use for critical rotating components such as blades and discs in the compressor stages was influential in the improvement of gas turbines during the latter part of the 20th century.
Fatigue methods based on life to crack initiation were originally employed for the design of critical disc and blade components. However, these approaches ignore any potential remaining life during which a crack may propagate in a sub critical manner. More recently, a more holistic approach to component lifing is used where the stages of crack initiation, through to short then long crack growth and final failure are considered. This approach requires a much greater understanding of the time independent (fatigue) and time dependent (creep) deformation and microscale damage, d_r and d_i respectively. Therefore, the total component damage, d_{total}, is given as

$$d_{total} = f(d_r, d_i) \tag{1}$$

Low temperature dwell effects in titanium alloys can be attributed to the phenomenon of strain accumulation over time observed in these alloys at ambient temperatures, loosely termed 'cold creep'[1,2]. Creep occurs in these alloys at low homologous temperatures (T/T_m<0.2), much lower than temperatures at which diffusion occurs. Consequently, time dependent deformation at ambient temperatures is not characterised by diffusion controlled mechanisms such as dislocation climb. Instead, creep occurs firstly by slip in grains favourably oriented for prism and basal slip.

Then, as these grains deform load is redistributed to neighbouring, less favourably oriented grains. Over time the internal stress distribution evolves to ensure compatibility and equilibrium is maintained between grains[3]. The limited number of slip planes combined with the relatively low levels of dislocation-dislocation interactions contributes to the low rates of work hardening observed in $\alpha+\beta$ titanium alloys such as Ti-6Al-4V. Low temperature creep is very dependent on microstructure [4]. Studies have shown that the α/β boundary in colony microstructures provides little resistance to the movement of dislocations from the α to β phase whereas misalignment between the slip systems in the α and β phase causes the formation of dislocation pile ups during slip transmission [5]

Another important factor in certain titanium alloys is that the accumulation of plastic strain at low temperatures may lead to premature fatigue failures, often characterised by subsurface crack initiation [6] and the onset of quasi-cleavage facets on basal slip planes in the hexagonal crystal structure [7,8,9]. These facets are not attributed to a brittle mechanism but to the gradual separation of slip damage concentrated within a persistent planar slip band [10], the formation of which is consistent with the variation on a Stroh pile up model, proposed by Evans and Bache[11] (figure 1). At low temperatures there is relatively little thermal energy available and dislocation pile ups readily occur at the grain boundaries where slip planes are misaligned. These pile ups facilitate the formation of quasi-cleavage facets on the basal plane of suitable orientated adjacent grains. Grains with a basal plane orientated perpendicular to the applied load are resistant to slip and are referred to as 'strong' grains. If an adjacent grain has favourably orientated slip systems then dislocations can pile up at the grain boundary. This pile up induces shear (τ_f) and tensile (σ) stresses in the strong grain which if sufficient will result in cleavage along the basal plane in the 'strong' grain. τ_s is the resolved shear stress in the 'weak' grain with σ_1 the stress applied to the system. This interaction between 'strong' and 'weak' grains is fundamental to the formation of quasi-cleavage facets and consequently the propensity for facet-dominated failures is related to alloy microstructure. Near α and $\alpha+\beta$ titanium alloys, such as Ti-6Al-4V, are particularly prone to cold creep/dwell effects[12].

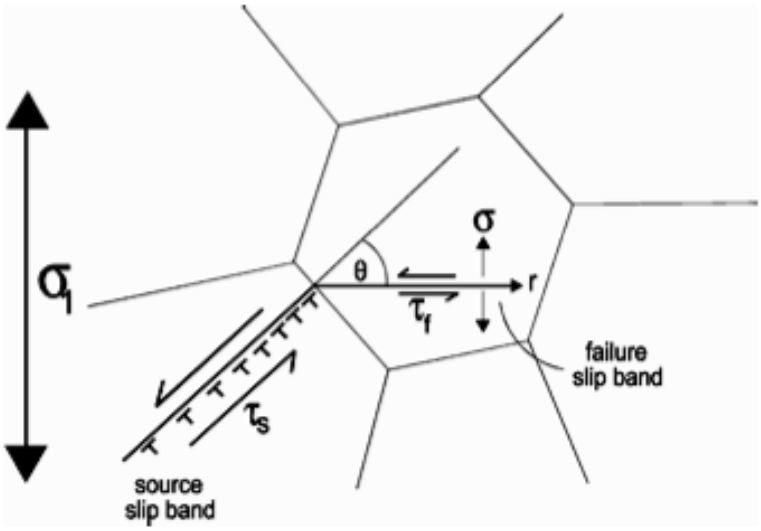

Figure 1: Mechanism of facet formation in titanium alloys.

Microstructures of titanium alloys are determined by composition and heat treatment in relation to the β-transus and cooling rates. Processing above the β-transus results in

substantial grain growth of the body centred cubic (bcc) β-phase. On cooling, the β-phase transforms to the hexagonal close packed (hcp) α-phase. Very fast cooling rates can result in martensite; however, cooling rates are usually sufficiently slow to allow diffusion and a needle-like basketweave microstructure forms. If the cooling rate is further reduced, as may be the case in thick sections, then a coarse, plate-like microstructure may form. These coarse microstructures are most susceptible to cold creep and thus dwell fatigue [12].

2. Experimental Procedure

Uniaxial creep tests were performed on Ti-6Al-4V at 20°C over a range of stresses. The specimens were machined from a forged disk displaying a random microstructure with predominantly equiaxed primary α grains shown in figure 2. The alloy had a primary α volume fraction of 60% with a primary α grain size of ~10μm.

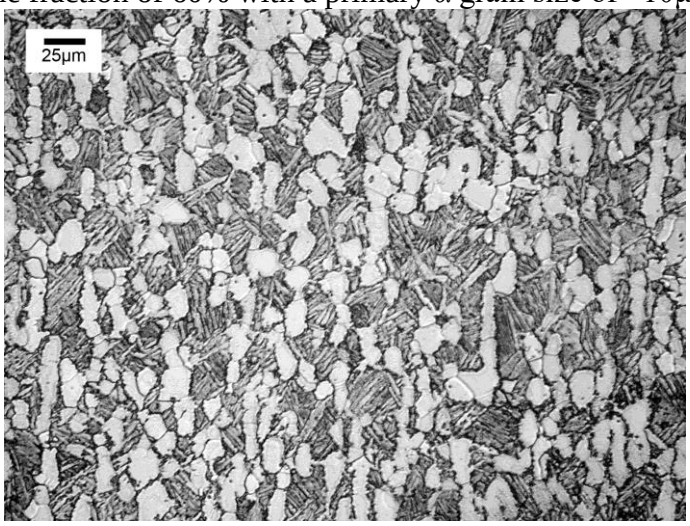

Figure 2: Micrograph of Ti-6Al-4V disk forging

2.1 The low temperature creep curve

A logarithmic relationship is often used to represent low temperature creep behaviour in many crystalline materials where little or no tertiary creep is observed[13].

$$\varepsilon_t = \alpha_1 \log_e \left(\alpha_2 t + 1\right) \tag{2}$$

where α_1 and α_2 are material constants, dependent on stress and temperature. α_1 quantifies the amount of primary creep whereas α_2 relates to the rate of decay of the creep rate. The creep rate at any given time can be given as

$$\dot{\varepsilon}_t = \frac{\alpha_1 \alpha_2}{\alpha_2 t + 1} \tag{3}$$

At low stresses, equation 2 is applicable to Ti-6Al-4V, however at ambient temperature, stresses above about 870MPa yield a poor fit is against experimental data for this alloy. At these stresses it was found that an additional term is required with a linear relationship with respect to time,

$$\varepsilon_t = \alpha_1 \log_e \left(\alpha_2 t + 1\right) + \alpha_3 t \tag{4}$$

where α_3 is a material constant dependent on both stress and temperature. This equation is shown graphically in figure 3. The rapid acceleration of creep rate prior to rupture is due to necking and is difficult to quantify numerically.

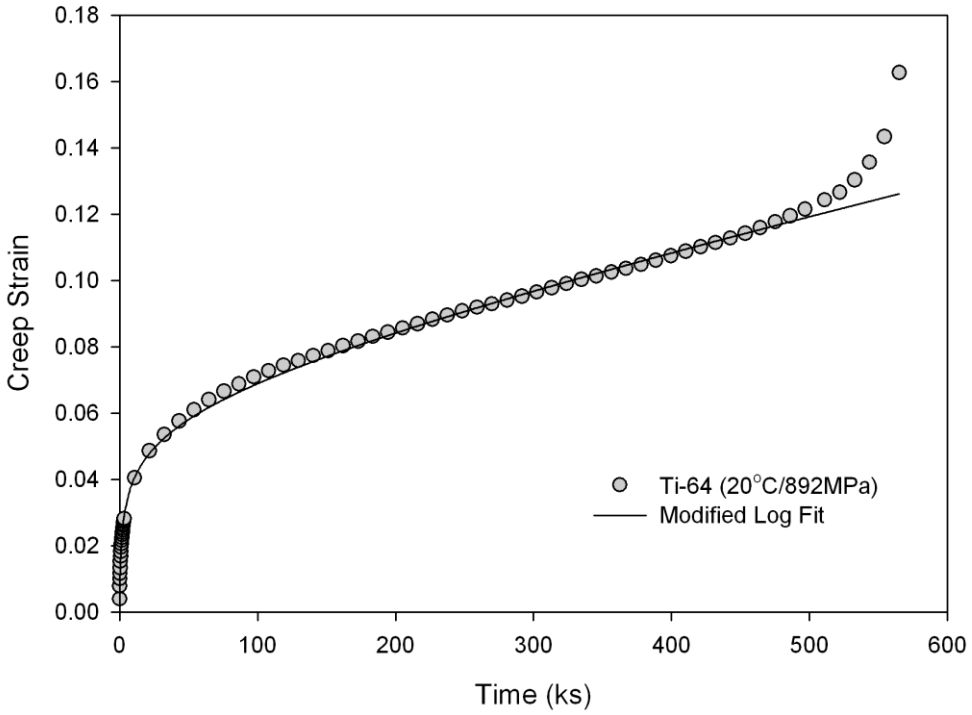

Figure 3: Ti-6Al-4V creep curve at 892MPa/20°C with fit using equation (4).

The creep rate at any given time then becomes

$$\dot{\varepsilon}_t = \frac{\alpha_1 \alpha_2}{\alpha_2 t + 1} + \alpha_3 \tag{5}$$

Since the first term on the right hand side of equation 5 provides the creep rate, $\dot{\varepsilon} \to 0$ as $t \to \infty$, α_3 is equal to the minimum creep rate $\dot{\varepsilon}_m$. It is proposed that this linear expression (α_3) could represent the quasi-cleavage faceting behaviour observed in Ti-6Al-4V explaining the deviation from normal log creep behaviour at high stresses.

2.2. The stress dependence of α_1, α_2 and α_3

On evaluating equation 4 against experimental creep curve data it was found that a power law expression could be used to represent the dependence of α_1, α_2 and α_3 with stress

$$\alpha_i = A_i \sigma^{n_i} \qquad i = 1,3 \tag{6}$$

where A_i and the stress exponent n_i (i = 1, 3) are material parameters which can be obtained by plotting $\ln(\alpha_i)$ against test stress. A linear trend line through the data gives n_i as the gradient and $\ln(A_i)$ as the $\ln(\alpha_i)$ intercept (figures 4-6). Values of 4.23×10^{-35},

4.39×10^{-152} and 1.74×10^{-288} were obtained for A_1 , A_2 and A_3 respectively and stress exponents of $n_1 = 10.9$, $n_2 = 50.6$ and $n_3 = 95.2$ were obtained.

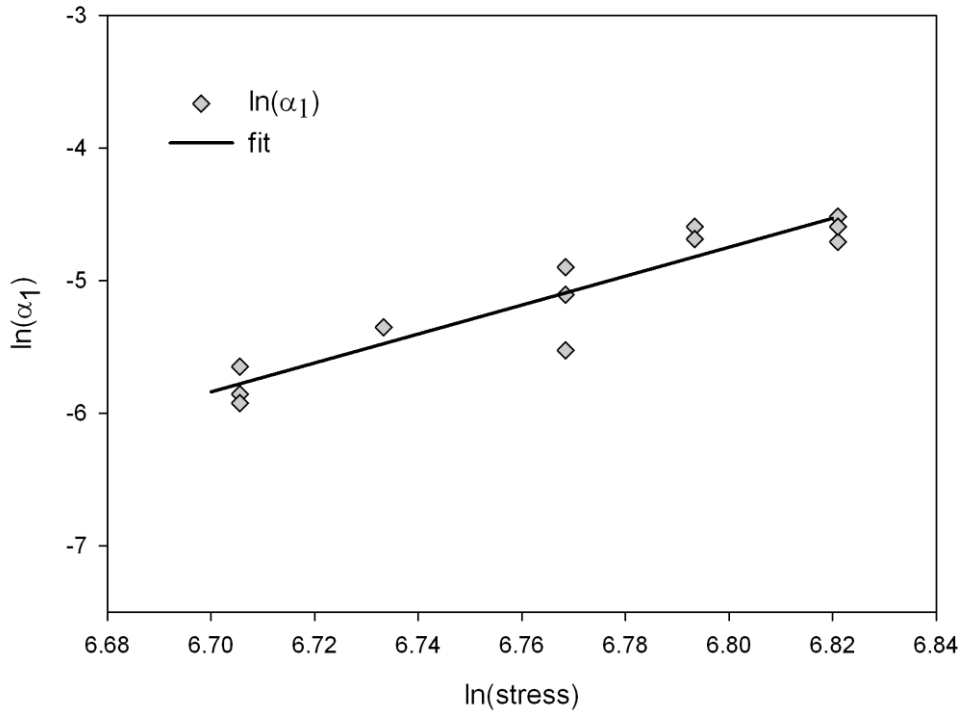

Figure 4: The variation of α_1 with respect to stress.

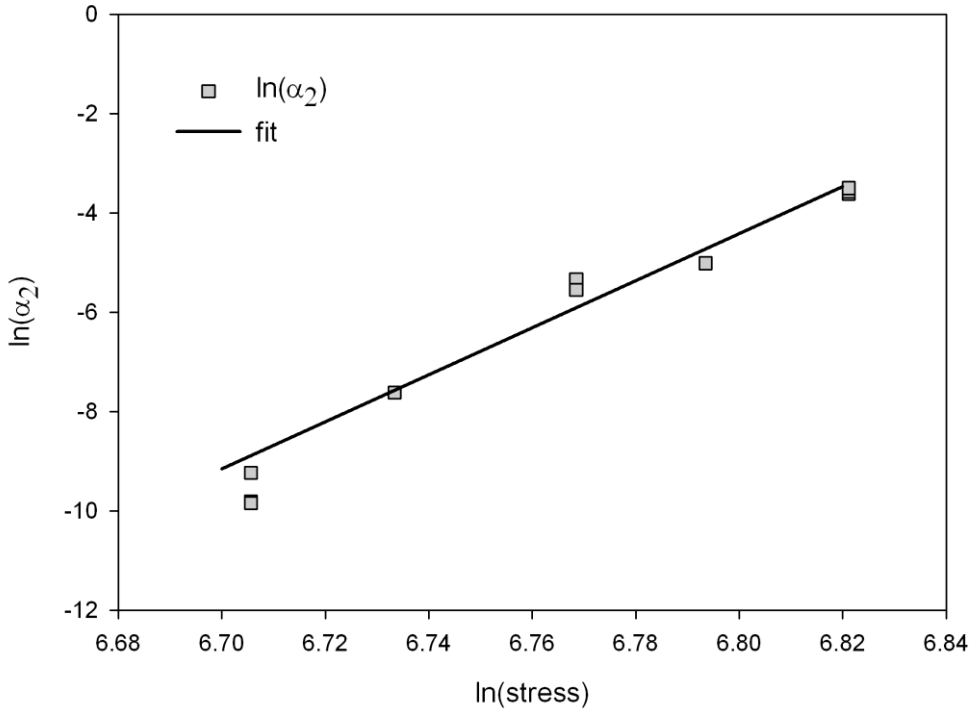

Figure 5: The variation of α_2 with respect to stress.

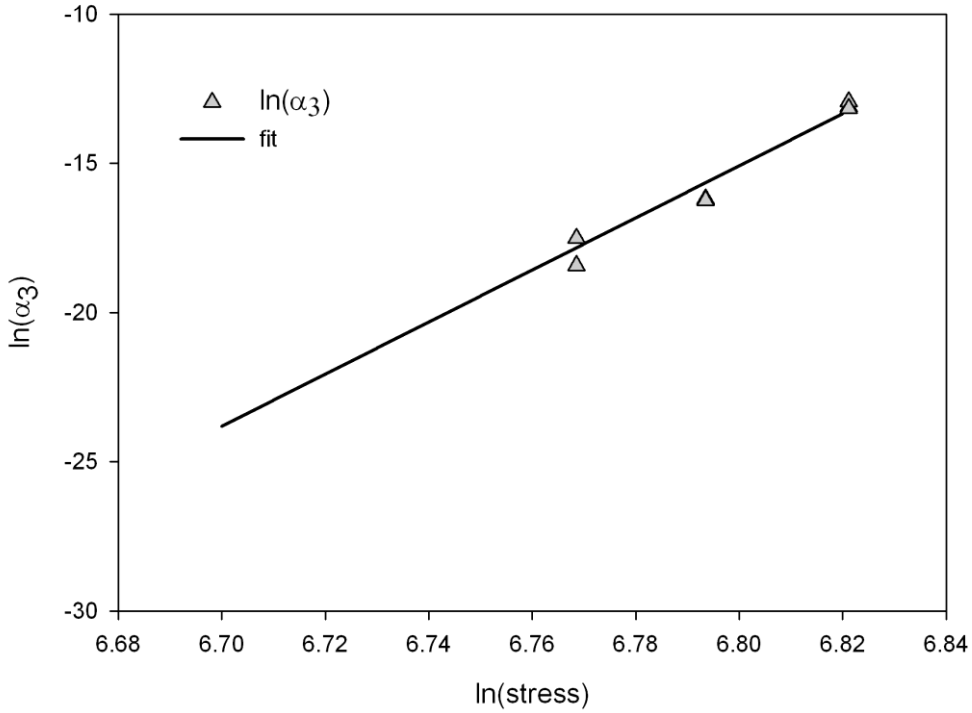

Figure 6: The variation of α_3 with respect to stress and temperature.

The above equations can be used to predict creep curves over a range of conditions at which cold creep occurs (figure 7).

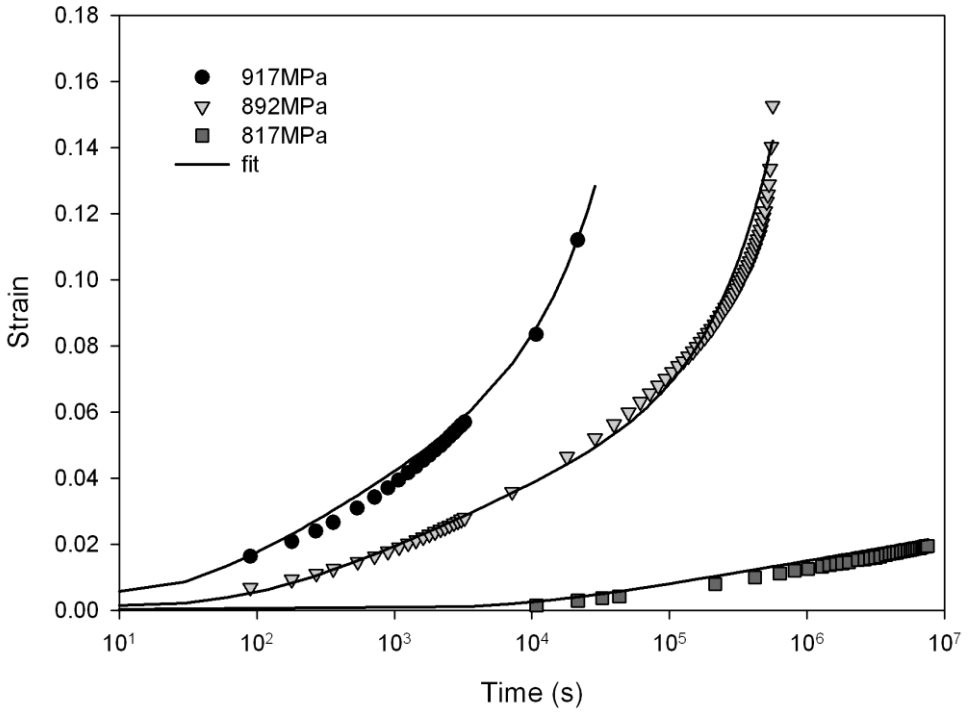

Figure 7: Predicted and experimental creep curves for Ti-6Al-4V at 20°C.

2.3. Cold creep rupture

At low stresses and at temperatures in the cold creep regime, creep rates of titanium alloys can continually decrease until a maximum strain is achieved and no rupture occurs. However, at higher stresses, at which α_3 becomes significant, creep rupture occurs due to the reduction in effective cross sectional area due to the formation of quasi-cleavage facets, an example of which is shown in figure 8. The time to creep rupture (t_f) can be expressed as:

$$\frac{1}{t_f} = A_f \sigma^{n_f} \tag{7}$$

Where A_f and n_f are material constants for cold creep rupture. These parameters can be obtained by plotting $\ln(t_f)$ against $\ln(\sigma)$ (figure 9). A stress rupture plot for Ti-6Al-4V at 20°C has a much shallower slope than at high temperature.

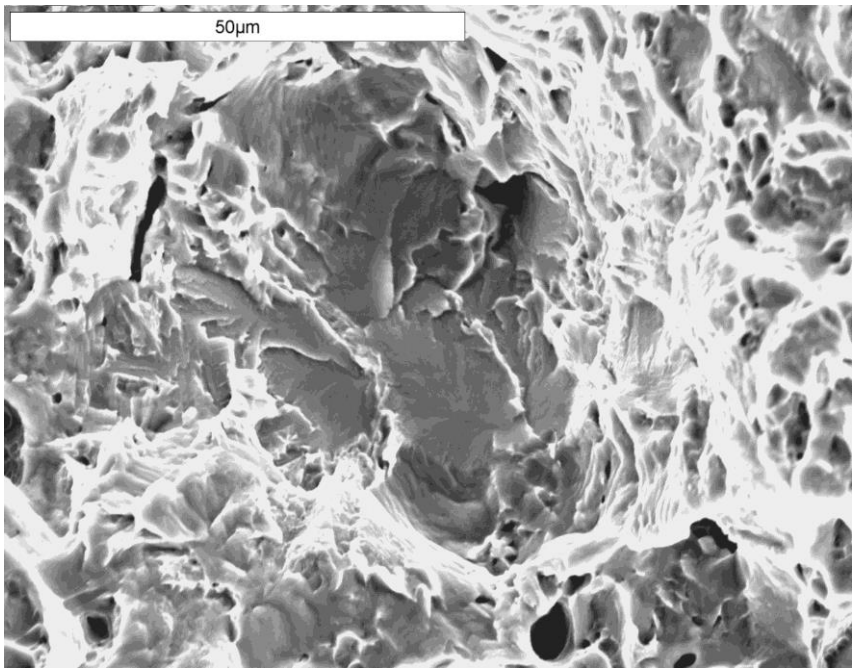

Figure 8: Quasi-cleavage facets in Ti-6Al-4V at 950MPa and 20°C.

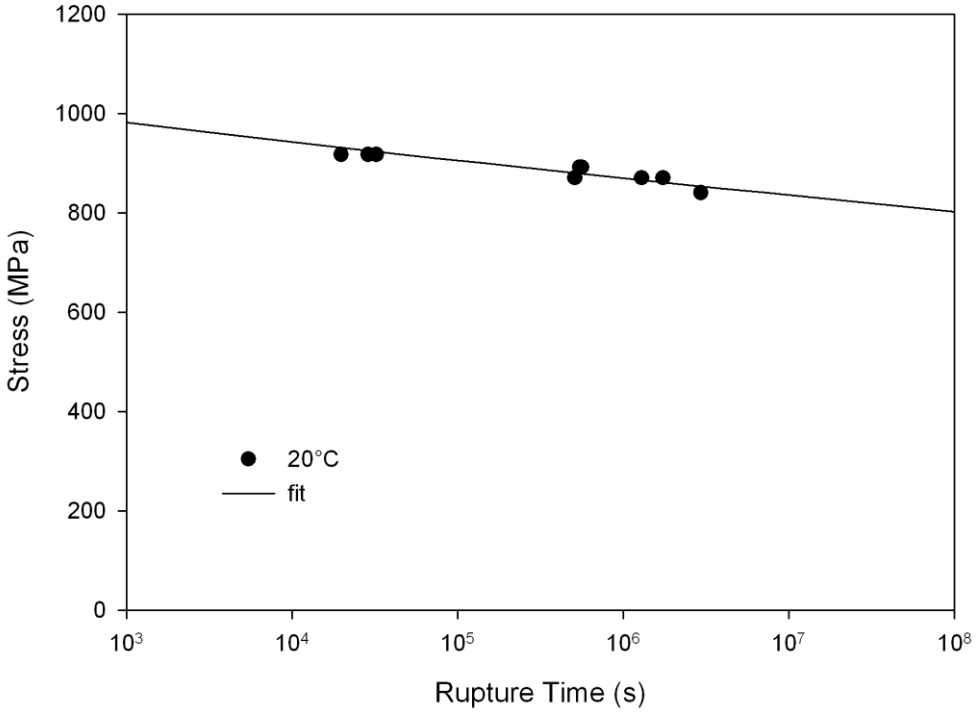

Figure 9: Stress/rupture time plot for cold creep in Ti-6Al-4V.

3. A finite element model for cold creep in Ti-6Al-4V

Equation 4 can be used to predict the cold creep rate at a given time. However when predicting creep in a component where the stress evolves with time, creep rate is dependent on prior creep and a suitable hardening model is required. Time-based hardening, although simple to apply is only accurate for cases where stress is relatively constant. A hardening model where creep rate is based on the total inelastic strain was found to be suitable for creep at ambient temperature.

$$\dot{\varepsilon}_c = f(\sigma, \varepsilon_i, T) \tag{8}$$

This method calculates creep rate using equation 5 where time, t, is substituted by effective time, t_{eff}, where t_{eff} is obtained by solving equation 4 with ε equal to the total inelastic strain. An Abaqus *CREEP subroutine has been compiled using this method.

4. Stress relaxation

An important requirement of a deformation model used for lifing high stress structures, such as gas turbine components, is its ability to predict stress relaxation behaviour since this will have a direct effect on the stress used for fatigue life calculations. Stress relaxation predictions for Ti-6Al-4V have been made with Abaqus using the method described above. The predictions have been compared to a uniaxial stress relaxation test for Ti-6Al-4V at 20°C completed in air. This test was conducted on a servo-hydraulic test machine using a MTS extensometer with a gauge length of 12mm and a specimen with a diameter of 6mm. Specimen strain was held at increasing values from 0.5% to 5% with stress allowed to relax for 1 hour at each

strain. A good correlation between predicted and experimentally obtained stress relaxation behaviour was obtained (figure 10).

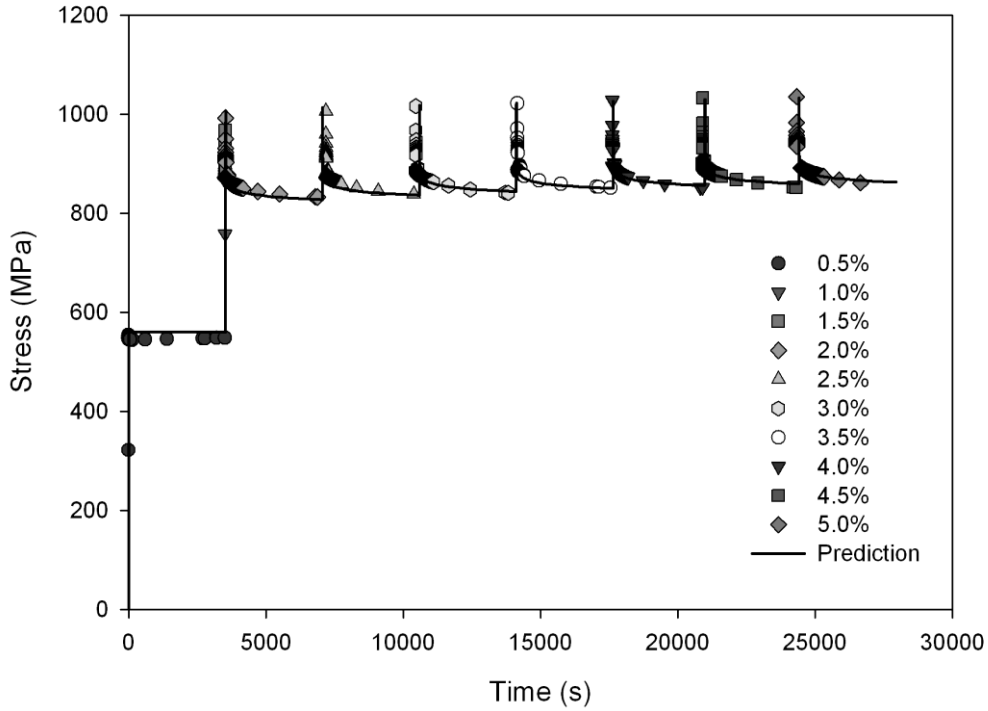

Figure 10: Predicted and experimental stress relaxation behaviour for Ti-6Al-4V at 20°C.

5. Fatigue behaviour of doubled-edge notched specimens

When predicting fatigue behaviour at any temperature, the time-dependent effect of creep should not be ignored, particularly if cycles with extended dwell periods at high stress or cycles with high mean stress exist. HCF lives of notched specimens with R = 0.8 show a distinct difference in trend when compared to those obtained with $R \leq 0.3$ and are characterised by the presence of cleavage facets. Therefore, it can be assumed that there is an additional failure mechanism other than that predicted using purely a fatigue lifing approach.

Abaqus finite-element analyses of these tests have been performed using the cold creep model described in this paper, with the addition of a creep failure criterion. A continuum damage parameter, ω, can be defined as:

$$\omega = t/t_F \tag{9}$$

where t_F is the creep rupture time calculated using equation 7. Creep failure in a region of material was assumed when $\omega \geq 1$ and a user defined field was used to reduce element stiffness once this failure criterion had been exceeded at each Gauss point in the element. Specimen failure was assumed when this failure criterion was exceeded in elements across the width of the section. Due to specimen symmetry a $1/8^{th}$ model was used with smaller elements around the specimen neck. Boundary conditions were applied along the faces which represent the lines of symmetry and a negative pressure was used to apply load to the model. The load was applied in a

cyclic manner between max and min values with an increasing interval as the analysis continued.

Specimen failure times predicted using this method closely correlate to test results with a rapid reduction in life with increasing stress (figure 11). A predicted path of rupture using this method is shown in figure 12. This figure shows the results of the FE model overlaid on a failed DEN specimen tested at 20°C with a peak elastic stress of 2000MPa. Both test and model exhibit failure at ~45° to applied stress. Specimen failure was assumed to occur once elements had failed across the entire cross section, however the time from crack initiation to final specimen failure was less than 2% of total specimen life. These results allow confidence in the ability of this model to predict time dependent effects in this variant of Ti-6Al-4V.

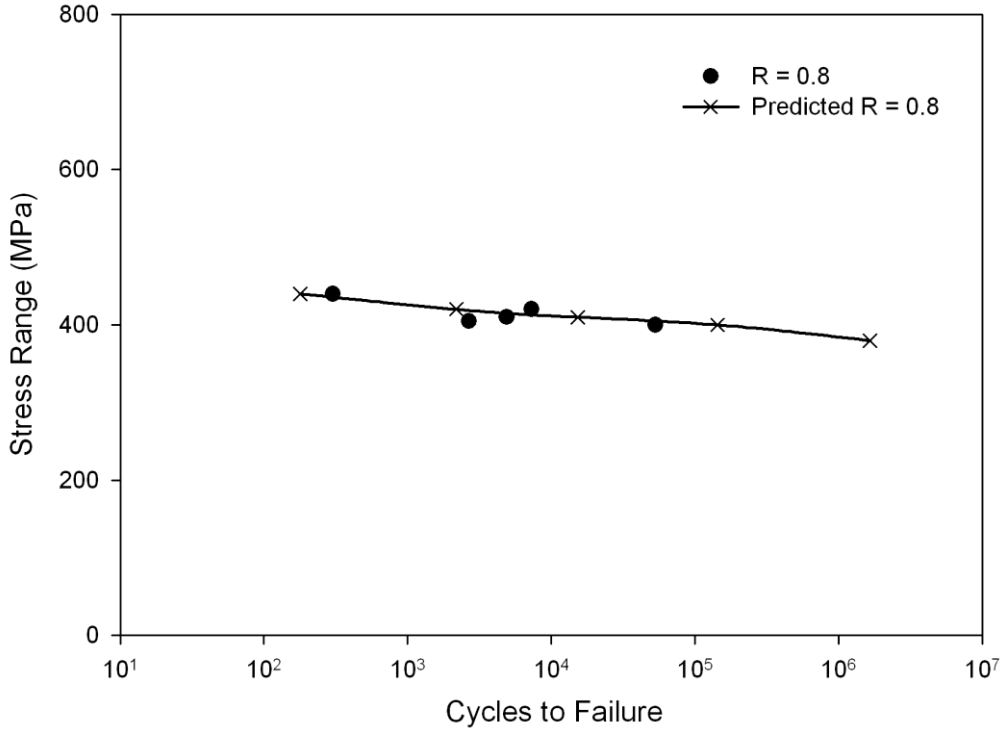

Figure 11: Fatigue lives of Ti-6Al-4V DEN specimens at 20°C with lives for R=0.8 tests predicted using the cold creep model.

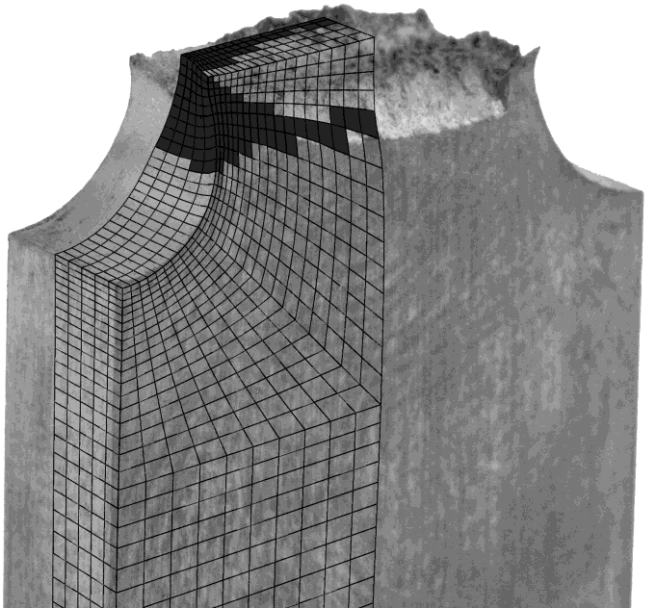

Figure 12: Fracture surface of a Ti-6Al-4V DEN specimen at 20°C, overlaid with a predicted path of failure (R = 0.8)

6. Discussion

The method described in this paper represents a novel approach to quantifying the effects of cold dwell in some titanium alloys. Moreover, the numerical parameters in the model characterise material behaviour. Low temperature creep is very dependent on microstructure and differences in material response will be reflected in the model parameters. A_1 and the stress exponent n_1 quantify α_1, the magnitude of primary cold creep strain. α_2 represents the rate of decrease in creep rate during the early stages of cold creep and is quantified by A_2 and n_2. Since the decrease in creep rate at ambient temperature is related to the rate of work-hardening, the model parameters A_2 and n_2 quantify the effect of the α+β microstructure on cold dwell.

Cold creep rupture occurs due to the onset of quasi-cleavage facets on basal slip planes in the h.c.p. structure. At stresses less than about 870MPa, creep rate decreases continuously and failure is unlikely. For these tests α_3 is negligible however, as stress increases the contribution of α_3 to the total creep rate becomes significant and failure is observed. For this alloy, the stress exponent of α_3 is high (n_3 = 95.2) meaning that as stress increases above 870MPa the effect of further increases in stress is significant. This is reflected in the low gradient observed in the stress rupture curve shown in figure 9. Since α_3 becomes significant at stress above which failure is observed, n_3 will represent the stress sensitivity of the microstructure to develop quasi cleavage facets.

The ability of the model to predict stress relaxation gives confidence in using this method to predict stress redistribution around a stress concentration feature thus aiding computationally based fatigue life calculations. Furthermore, the model may be used to predict component failure where stress levels are below that required for static failures at ambient temperatures.

7. Conclusions

- A numerical method for predicting ambient temperature creep and creep rupture of Ti-6Al-4V over a range of stresses has been derived.
- An Abaqus user defined creep model has been developed based on this method. This model relates creep hardening to total inelastic strain.
- This model has shown to be accurate for predicting stress relaxation behaviour of Ti-6Al-4V at 20°C.
- Finite-element analyses of DEN specimens under cyclic load have been used to predict the lives of R = 0.8 HCF tests based on a continuum damage method.

References

[1] H. Adenstedt, Met. Prog. 56 (1949) 658–660
[2] N.C. Odegard, A.W. Thompson, Metall.Trans. A 5 (1974) 1207.
[3] V. Hasija, S. Ghosh, M.J. Mills, D.S. Joseph, Acta Mater. 51 (2003) 4533–4549.
[4] W.H. Miller Jr, R.T. Chen, E.A. Starke Jr, Met. Trans. A 18A (1987) 1451.
[5] S. Suri, G.B. Viswanathan, T. Neeraj, D.-H. Hou, M.J. Mills, Acta Mater. 47 (1999) 1019-1034.
[6] G.F. Harrison, P.H. Tranter, M.R. Winstone, W.J. Evans, Designing with Titanium, The Institute of Metals, London, 1986, 198–204.
[7] M.R Bache, M Cope, H.M Davies, W.J Evans, G Harrison, Int. J. Fat. 19 (1997) 83-88.
[8] M.R Bache, H.M. Davies, W.J. Evans, in: P.A. Blenkinsop, W.J. Evans, H.M. Flower (Eds), Eighth World Conference on Titanium, Birmingham, October 1995, Titanium 95, The Institute of Materials, London, 1996, pp. 1347-54.
[9] M.R. Bache, Int. J. Fat. 25 (2003) 1079–1087.
[10] W.J. Evans, M.R. Bache, Int. J. Fat. 16 (1994) 443-52.
[11] W.J. Evans, M.R.Bache, Fatigue Behaviour of Titanium Alloys, The Minerals, Mining and Materials Society, 1999, pp99-110.
[12] W.J. Evans, Fatigue Fract Eng Mat Struct, 27 (2004) 543-557.
[13] R.W. Evans, B. Wilshire, Creep of Metals and Alloys, The Institute of Metals, London, 1985.